5.1 Introduction

With the emergence of nanoscience and nanotechnology, several new strategies for designing nanoscale materials have been developed [272]. In line with this, Metallic nanoclusters have emerged as promising new nanoscale materials with numerous applications in the healthcare system [14]. Conventional nanomaterials include silver, zinc, nickel, titanium, and copper, which are non-biological in origin and semiconductors, which are larger in dimension and constitute toxic elements that cause toxicity due to accumulation in the system [100] also their potential in nanomedicines, agriculture, and food sectors is hindered by their lack of biocompatibility, non-degradability, and function as a generator of nano waste [74].

The alkaline earth metal-based nanomaterials are a suitable alternative approach for bioimaging and biolabeling applications due to their compatibility towards biological systems and useful degradation products (Mg, Ca ions) for the body [74,75,88,166]. The Mg-based nanomaterials have been recognized as a safe alternative with extraordinary activities by the U.S. Food and Drug Administration (FDA) [74]. Because of their strong optical and electrical band gap, thermodynamic stability, low dielectric constant, and low refractive index, MgNCs have proven to be a stable and desirable material [186]. Apart from magnificent characteristics, very few attempt has been carried out to synthesize calcium and magnesium-based nanomaterials due to their prosperity toward making oxides owing to their lower reduction potential [3]. For the industrial fabrication of magnesium nanomaterials, the most common methods such as ultrasonication, microwave irradiation, wet impregnation, laser-vaporization pathways, sol-gel, and hydrothermal methods were deployed [12,94,113]. But the use of toxic chemicals and solvents in the production of Mg-based NCs raises their toxicity and pollutes the environment. However, physical procedures

necessitate a lot of energy, rendering them less cost-effective than alternative ways and resulting in the production of non-homogenous particles. [74]. On the other hand, greener synthesis or utilization of bio reductants as an alternative of hazardous chemicals could tend to be cost effective, biocompatible and environmental friendly [67]

In line with this, Shivesh et.al.[183] have reported biocompatible calcite nanoclusters for bioimaging applications, but the reported quantum yield is relatively low (0.1%), whereas large-size magnesium nanoclusters have been synthesized previously by Pandya et al. and Juhi et al. via a chemical reduction route by utilizing BSA protein [3,85]. while their MgNPs fluoresce only in the blue-green regimes and utilize as artificial nanozyme respectively. It would be of great interest to develop highly fluorescent magnesium nanomaterial with red emission that could be able to penetrate tissue in-depth and also minimizes background fluorescence [171].

Hen egg white lysozyme (14.3 kDa) protein is a highly stable, easily available, and water-soluble protein with 129 amino acid long chain constituting eight cysteine residues. Additionally, its identical tertiary structure makes a good template for wide applications such as sensing, imaging, and self-assembly [176,220,273]. L-Ascorbic acid (AA) is a common water-soluble vitamin, which is a crucial ingredient for various essential hydroxylation reactions [93]. For combating bacterial infections, AA plays a pivotal role by acting as a potent reducing and antioxidant agent. In our study, AA acts as stabilizing agents toward the synthesis of Lyz-MgNCs [175,274].

Herein, we reported a simple facile one-pot synthetic protocol using commercially available reagents lysozyme protein and L-ascorbic acid for the development of multifluorescent magnesium nanoclusters at moderate temperature using water as a solvent medium. Prepared clusters exhibited high quantum yield in both blue and green regimes.

Our reaction procedure is similar to the biomineralization process of organisms in nature; we assumed that at 55 ºC temperature, lysozyme unfolded and the negatively charged functional groups attached to magnesium ions via electrostatic interaction. The reduction capability of a lysozyme protein was activated by maintaining the reaction medium pH close to 12. The entrapped Mg ions underwent a progressive reduction process to turn magnesium NCs in situ, further ascorbic acid involvement facilitated surface modification of Lyz-MgNCs surface and besides providing biocompatibility and hydrophilicity also tend to enhance the fluorescence capacity of Lyz-MgNCs. Furthermore, it was scientifically proven that ascorbic acid binds to the partially unfolded lysozyme and stabilizes it, as well as prevents further conformational changes [275]. Hence, ascorbic acid has great potential for stabilizing and enhancing hydrophilicity of lysozyme-templated nanoclusters [274–276].

5.2 Materials and Methods

5.2.1 Chemical reagents

High-grade, 99.9 % pure Magnesium chloride salt ($MgCl_2$) and L-ascorbic acid were purchased from Sigma Aldrich. High-quality hen egg white lysozyme (HEWL) and sodium hydroxide pellets (NaOH) were purchased from SRL private limited. Ultrapure deionized water was utilized throughout the reaction process, and all the mentioned chemicals were used without any adulteration and purification.

5.2.2 Synthesis procedure

All the glass wares were washed with aqua regia before performing the reaction. Briefly, $MgCl_2$ salt (10 mM) and lysozyme (50 mg) were mixed in deionized water, and the solution was stirred for 5 minutes at 55 ºC, and then 0.05 mL NaOH (1M) was added to maintain the pH close to 12.

Afterward, 35 mg/ml L-ascorbic acid was added, and the resulting solution was stirred for 2 h at 55ºC followed by incubation for 24 hrs. During the entire course of the reaction, the conical flask was tightly sealed with cotton plague and parafilm wrap. After 24 h of incubation, the solution color changed from colorless to pale yellow. Prepared yellow colored solution centrifuged at 15k rpm for 5 min in order to remove larger particles and unreacted ligands. The same synthesis procedure was followed for all possible controls.

5.2.3 Characterization

Size estimation of Lyz-MgNCs was performed using an FEI Tecnai G2 20 TWIN transmission electron microscope (TEM) with an accelerating voltage of 200 kV. The 10-fold diluted sample of Lyz-MgNCs was drop casted onto carbon coated coper grid and allowed to air dried in room temperature. Fluorescence spectra and UV-Vis absorbance spectra were recorded using PTI Quanta master 400 (Slit width = 1 nm, integration time = 0.1s and step size = 1nm) and using Elico SL210 spectrophotometer, respectively. Circular dichroism (CD) spectra of native protein and Lyz-MgNCs was conducted using JASCO CD Polarimeter J-1500 at 25º C temperature within a holder of 10 mm path length, Fourier transform infrared (FTIR) spectroscopy were conducted using Nicolet iS5, THERMO Electron Scientific Instruments LLC instrument in the range of 400-4000 cm-1. X-ray diffraction (XRD) and X-ray photoelectron spectroscopy (XPS) were carried out using Rigaku Miniflex 600 Desktop X-Ray Diffraction System (RIGAKU Corporation) and K-Alpha (Thermo Fisher Scientific) instruments respectively. cellular imaging studies on brain cells were performed using Leica microsystem, model SP8 STED. whereas, quantum yield calculations were performed on Horiba PTI Fluorescence Quanta Master 400 Systems, and absolute quantum yields (QYs) of the synthesized nanoclusters were achieved using a PTI K - Sphere petite Integrating sphere. In vivo fluorescence imaging system

(Photon Optima Imager, manufactured, Biospace, France) used to harvest fluorescence signal.

5.2.4 Cell culture and incubation with Lyz-MgNCs for bioimaging application

The cytoplasmic uptake of Lyz-MgNCs in U-87 MG cells was examined by using confocal microscopy in the blue, red and green regimes. U-87 MG cells were seeded onto coverslip containing two different 6 well culture plate in complete medium with a density of 2×10^5 cells per well. After 24h, the seeded cells were treated with 1/10 ratio (Stock Solution -12.4 mg/ml) of freshly prepared Lyz-MgNCs nanoclusters with the complete medium and incubate further for 24 hrs at 37 ºC in humidified atmosphere of 5% CO_2 incubator. After 24 hrs, the adherence cells on coverslips were took gently from each well and finally the cells were fixed by using 4% formaldehyde and dabco and visualized under confocal microscopy to study the cytoplasmic fluorescence property of nanoclusters.

5.2.5 Cytotoxicity evaluation

The cytotoxicity of cells treated with magnesium nanoclusters was measured using a colorimetric assay based on the reaction of the yellow tetrazolium salt MTT (3-(4, 5-dimethylthiazol-2-yl)-2,5-diphenyl tetrazolium bromide) with the mitochondrial succinate dehydrogenase of metabolically active cells, yielding purple-colored formazan crystals. Proliferation of U-87 MG cells was measured after being exposed to magnesium nanoclusters and control vehicles. The cell line was grown at 37 ºC in a humidified 5% CO_2 atmosphere in high glucose complete DMEM (complete media consisting of 10% FBS, supplemented with 20 mM L- glutamine, 100 units/mL penicillin, and 100 g/mL streptomycin). Adherence was tested by seeding 1×10^6 U-87 MG cells in each well of two separate 96-well plates and incubating them for 24 hrs.

When the initial medium had been incubated for 24 hrs. at 37ºC in a 5% CO_2 humidified atmosphere, it was discarded and replaced with fresh DMEM containing varied concentrations of distinct Lyz-MgNPs (1/10 th, 1/100 th, 1/1000 th concentrations of 12.4 mg/ml stock). After removing the media, 5 mg/mL MTT solution in 100 L of fresh medium was added to each well, and the plates were incubated for an additional 2 hrs. After 30 minutes of incubation in the dark at 37 ºC, the MTT solution was discarded and 100 L of DMSO was added to each well to dissolve the formazan crystal. Micro ELISA plate readers set to 570 nm measured the generated colour's intensity [277] .This formula was used to calculate an approximate cell viability:

% Cell viability = [O.D of nanoclusters treated cells/O. D of Control cells] ×100

5.2.6 Blood Compatibility assay

The safety of Lyz-MgNCs in the blood of healthy subjects was evaluated by haemolytic analysis. After centrifuging the sediment red blood cells were rinsed with PBS. In an Eppendorf microtube, 0.2 ml of washed blood and 0.8 ml of Lyz-MgNCs (diluted in saline) were mixed for 2 hrs with moderate shaking for 30 minutes. After incubation, the samples were centrifuged for 10 minutes at 2000 rpm. The supernatant was then poured into the 96-well plate at a volume of 100 µl. An absorbance measurement was taken at 570 nm, which is considered the maximum absorption wavelength. The positive control taken was distilled water, whereas the negative control was PBS. The percentage of the haemolysis was determined by the following equation:

$$\textbf{\% Hemolysis} = [(Abs\ T - Abs\ C)/(Abs100\ \% - Abs\ C)X100]$$

Here AbsT is the supernatant absorbance of the nanoparticles-incubated samples, AbsC is the negative control supernatant (PBS) absorbance, and Abs100 % is the positive control supernatant absorbance.

5.2.7 Histopathology in rat

Healthy rats of both sexes weighing between 200-250 grams were obtained and housed under natural conditions with a temperature of 25 ± 2 °C and 50-60% relative humidity. They were provided with full-price nutritional pellet feed and sterile water ad libitum for a period of 4-5 days before the start of the experiments. After one week of acclimatization, Charles Foster (CF) rats weighing 250 ± 20 grams were randomly divided into two groups, with nine rats in each group (n = 9). Group 1 received an intravenous injection of normal saline through the lateral tail vein, while Group 2 received an injection of Lyz-MgNCs. Histopathology studies were conducted on vital organs such as the brain, lungs, liver, kidneys, and spleen of the rats. The rats were treated with saline (control), Lyz-MgNCs (dosed at 70 mg/kg), and were euthanized at three different time points: 3 hours, 7 days, and 28 days post-treatment. Three rats were euthanized at each time point, and their organs were collected for histopathological analysis. The collected organs were washed with a saline solution, fixed in a 10% formalin solution, and embedded in paraffin. Paraffin sections of 5 μm thickness were then cut and mounted on glass slides. After staining with hematoxylin and eosin (HE) for cytoplasmic contrast, the sections were examined under a light microscope to observe any histopathological changes.

5.2.8 Clinical signs and body weight measurement

Rats (250 ± 20 g) were randomly segregated into the two groups (n=3). The first group will receive the normal saline (control group) and second group will receive the Lyz-MgNCs dissolved in the saline. Animal appearance, activity, hair, probable trauma, feces and mortality were observed before and 0–3 h after administration of the Lyz-MgNCs. Weight change, an important toxicity index for rats, was measured before dosing and after dosing

of 0.5 ml of the Lyz-MgNCs at the interval of 2 nd day, 7th day and 28 days. No differences were observed within dosing groups as compared to control.

5.2.9 In vivo biodistribution of the Lyz-MgNCs in the healthy mice

The aim was to investigate the biodistribution of Lyz-MgNCs in live Swiss albino mice. In this study, 50 µL (12.4 mg/ml stock) of Lyz-MgNCs solution was injected through the tail vein of healthy mice. Fluorescence imaging of the mice was conducted 3 hours after injection using an in. The mice in the control group did not receive any intravenous injections. The data obtained from the study was analyzed using M3Vision software to draw conclusions and insights [46,278].

5.2.10 Absolute Quantum Yield Measurement

For computing the absolute quantum yield of Lyz-MgNCs (absorbance value <0.5) at blue and green region, the sample and blank (DI water) filled 1 cm conventional quartz cuvette was mounted at the center of the integrating sphere to maximize the interaction of incident light with the sample. The integrating sphere collects all of the light emitted and dispersed by a fluorescent sample. Different excitations were applied to samples using a 75 W Xe PTI arc lamp housing (A-1010 B). Comparing the corrected emission spectra of a standard dye, Rhodamine 6G (in ethanol = 0.95) determined with the integrating sphere configuration to the corresponding spectra obtained with a calibrated spectrofluorometer was used to determine the accuracy of the spectral correction [279].

5.3 Result and discussion

Herein, a simple facile one-pot method was utilized to reduce magnesium chloride salt by using lysozyme and ascorbic acid at pH 11-12 in 55°C with constant vigorous stirring for 2 h. The solution medium, after 24 hrs of incubation, appeared pale yellow and give intense

blue, green and red colour under fluorescence spectrophotometer. Moreover, lysozyme is a non-toxic, biodegradable, and readily available antibacterial enzyme, which are animal derivative. Therefore, this rapid and yet simple method of preparing water-soluble, highly fluorescent Lyz-MgNCs could be adopted for large-scale production of Lyz-MgNCs required for commercial applications[176,274].

The UV−vis absorbance spectrum of the prepared Lyz-MgNCs did not exhibit any peak in the region 400−800 nm (Figure 5.1d), thus excluding the formation of SPR particles. However, the lysozyme protein spectrum consisted of peaks at 280 nm which corresponds to aromatic residue [277]. The hypochromic shift (280→264) in lysozyme templated Mg attribute the peaks to the formation of Mg-thiolate complexes, either as independent species or on the surface of Mg atoms [33,43]. Using fluorescence spectrofluorometer, the fluorescence spectra of Lyz-MgNCs and their controls were acquired. The aqueous suspension of Lyz-MgNCs exhibited emission spectra at 450 nm (blue), 545 nm (green), and 628 nm (red) at excitation wavelengths of 366, 469, and 560 nm, respectively (Figure.5.1). These sharp spectra are indicative of successful development of fluorescence Lyz-MgNCs. The control experiment in the absence of $MgCl_2$ salt also indicated the presence of fluorescent species (Figure.5.1) due to the presence of chromophore residue in lysozyme protein however, the intensity of fluorescence was small and they are insignificant to stain cells.[220] (Appendix – Figure. C1)

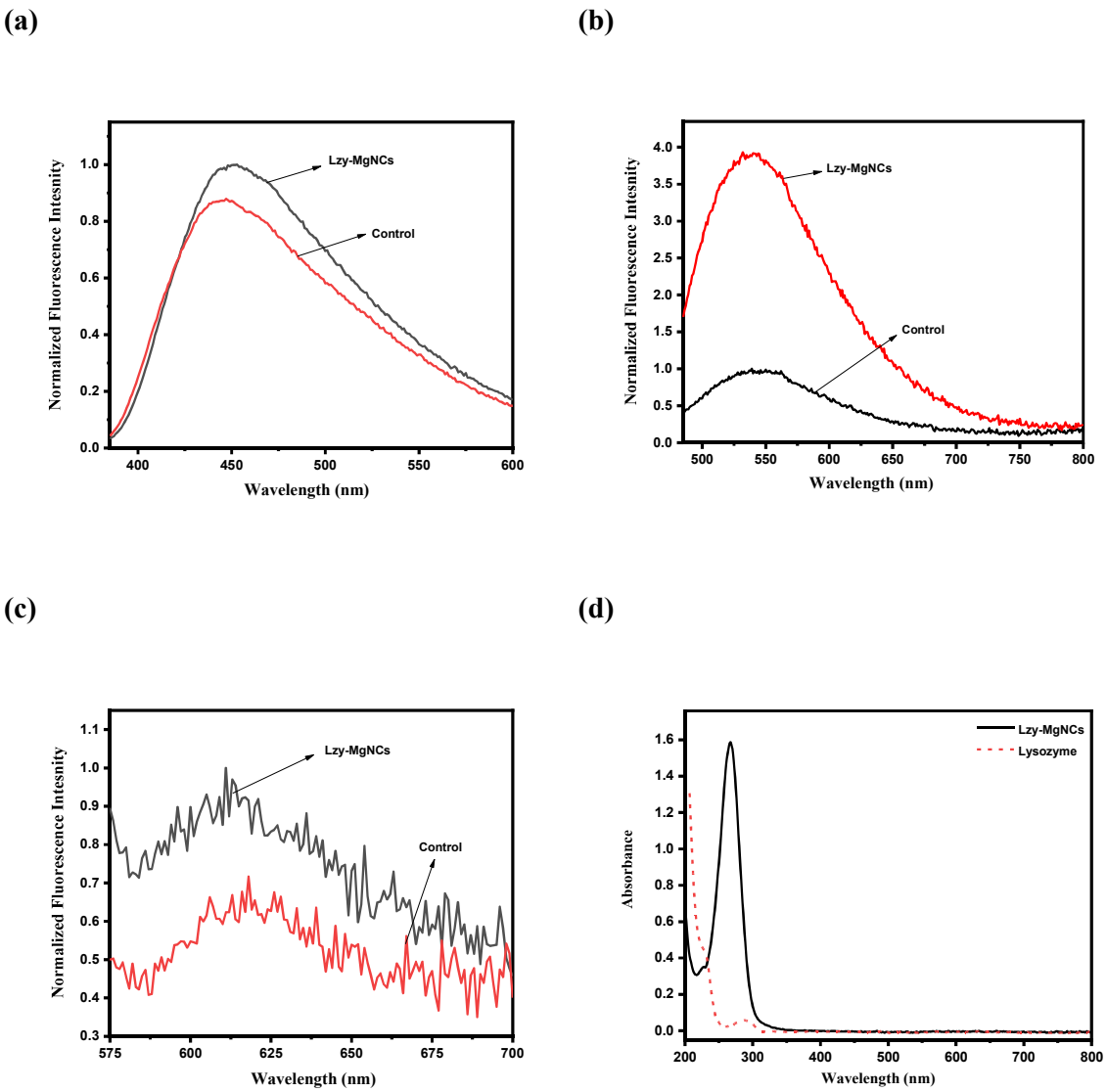

Figure. 5.1 The fluorescence emission spectra of Lyz-MgNCs and its control (without salt) (a) The optimal excitation emission spectra of Lyz-MgNCs and control at Ex- 366 / Em- 450 (b) The optimal excitation-emission spectra of Lyz-MgNCs and control at Ex- 469 / Em- 545 (c) The optimal excitation-emission spectra of Lyz-MgNCs and control at Ex- 560 /Em- 628(d) UV spectroscopy of Lyz-MgNCs and native Lysozyme.

In addition, High resolution transmission electron microscopy (HR-TEM) analysis of the as-prepared Lyz-MgNCs (Figure. 5.2 a) revealed the formation of spherical nanoclusters with nearly uniform size distribution (Figure. 5.2 b). The average diameter calculated from

20 points of these particles was determined to be 4 nm. Crystal lattice fringes with 0.28 nm spacing indicates the (100) planes of the metallic Mg [85] (Figure. 5.2 c (inset)).

X-ray diffraction peaks of Lyz-MgNCs revealed the crystalline nature of the Lyz-MgNCs and aligned with the face-centered cubic structure of metallic magnesium (Figure. 5.2 d). The XRD pattern contains multiple sharps peaks which are clearly remarkable. XRD spectra of prepared Lyz-MgNCs match with diffraction patterns of hexagonal Mg (JCPDS 04-0770). Peaks observed at 2θ = 27.4°, 31.6°, 45.3°, 56.4°, 66.1° and 75.2° are assigned to the (001), (100), (102), (110), (202) and (104) planes of hexagonal magnesium, respectively and similar with previously published reports [85]. No significant diffraction peak is observed for magnesium oxide (MgO) phase (JCPDS 89-7746) or any other magnesium phase except hexagonal Mg indicating that the product prepared via this route is single phase metallic magnesium [85].Further, the absolute quantum yield of the NCs was measured to be 5% (at 366 nm), and 6.8% (at 469 nm). This is comparable to the reported emission efficiency of Lyz-MgNCs and thus indicated the generation of strongly emitting particles [273].

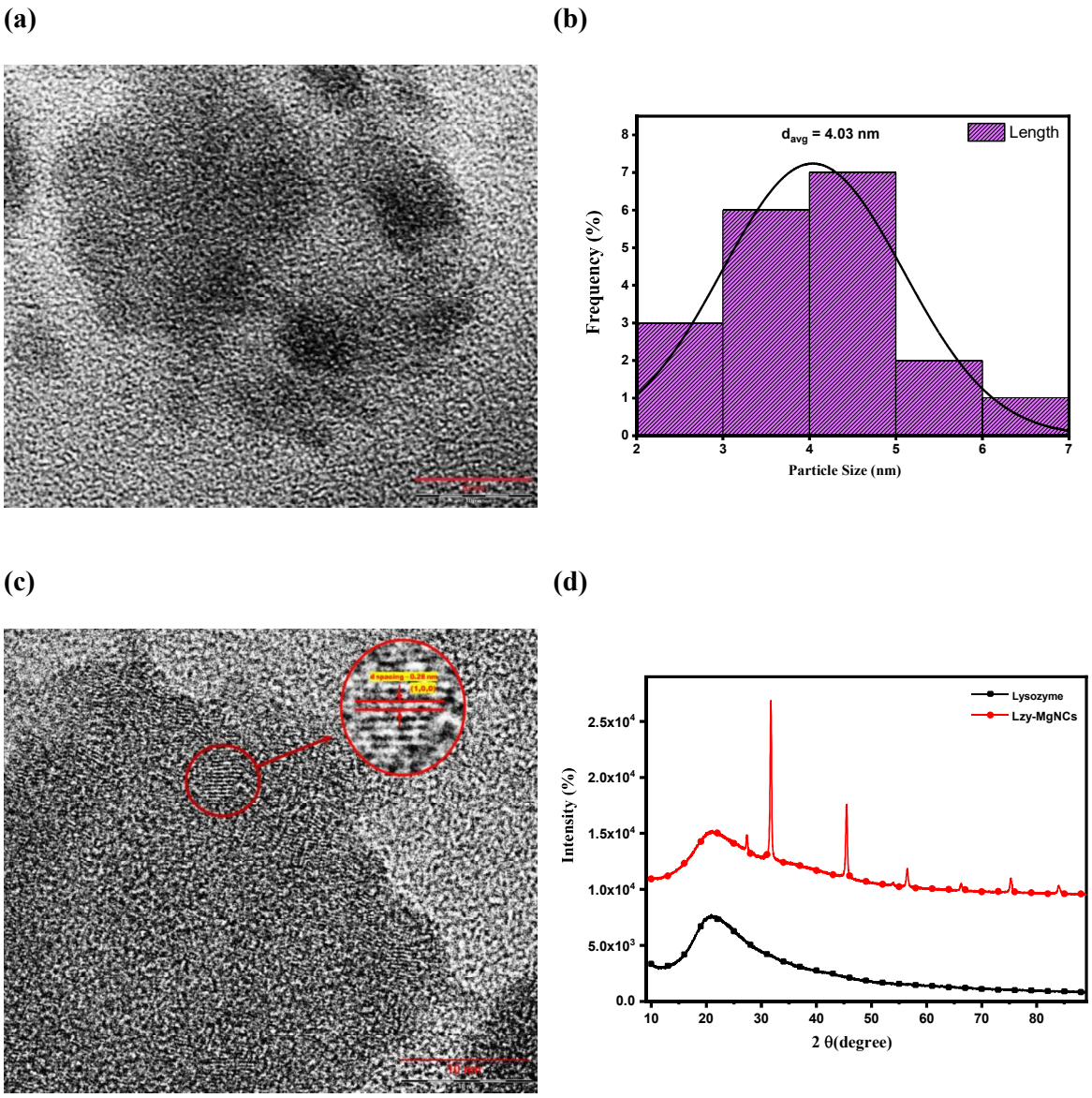

Figure. 5.2 (a) HR-TEM image of the Lyz-MgNCs at 20 nm scale bar (b) Particle size distribution curve, which was calculated using TEM image. (c) Observed diffraction pattern and d-spacing of Lyz-MgNCs (d) XRD spectra of Lyz-MgNCs and native lysozyme protein.

The FTIR spectra of lysozyme and lysozyme-stabilized Lyz-MgNCs are shown in (Figure. 5.3 a). In the spectra, three amide bands (amides I, II, and III) due to the protein occurred at 1600-1700, 1429-1575, and 1229-1300 cm^{-1}, respectively. Moreover, the spectral peaks at 3400-3000 cm^{-1} due to NH and OH stretching vibrations were prominent. Lyz-MgNCs may be stabilized by the presence of functional groups such as NH_2, COOH, and SH in the lysozyme protein. In a highly alkaline environment, the protein may have partially unfolded, exposing a sufficient number of these groups to facilitate the attachment of the NCs to the protein. It is also possible that the protein's three-dimensional structure, with its functional groups separated spatially allows for the attachment of multiple clusters to the same protein [183,220,280].

Circular dichroism study further confirmed the alterations in conformation of lysozyme caused by the reduction of an alpha helix. At 25 °C, the CD spectra of purified lysozyme and lysozyme-templated Lyz-MgNCs were measured in the wavelength range of 190 nm to 260 nm [9]. The lysozyme spectrum contains two bands at 208 nm and 222 nm, these bands are indicative of the p-p* and n-p* transitions in a helix. Lysozyme and Lyz-MgNCs were found to contain 50 % and 42% a helix, respectively. which demonstrate a drastic alteration in the lysozyme secondary structure subsequent to the formation of Lyz-MgNCs [220]. (Figure.5.3 b)

(a) **(b)**

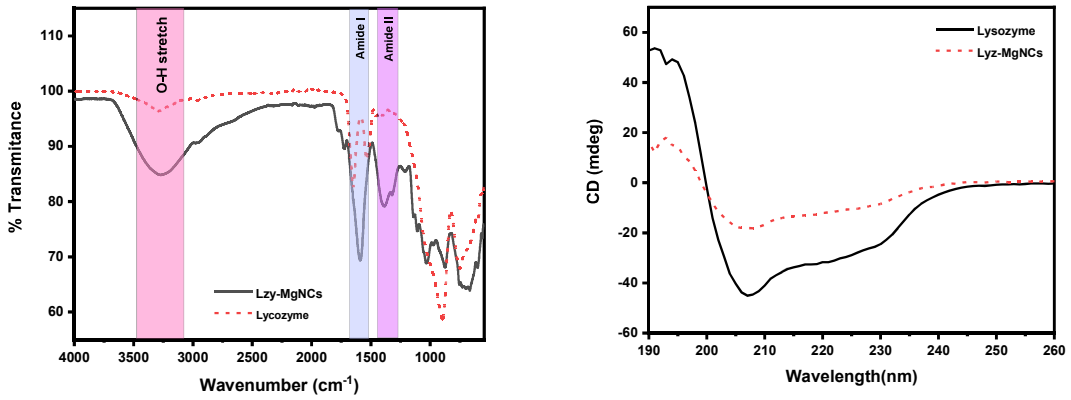

Figure. 5.3 (a) FTIR spectra of Lyz-MgNCs and native lysozyme protein (b) CD spectra of Lyz-MgNCs and native lysozyme protein.

Magnesium is the most readily oxidized metals due to its low reduction potential. Therefore, determining the oxidation state of Mg in the composite was considered essential. To corroborate the oxidation state of Mg in the Lyz-MgNCs samples, XPS analysis was carried out. One broad prominent peak observed at 1303.7 eV were assigned to Mg1s, which were characteristic peak of metallic magnesium (Mg^{o}) [281–283] (Figure. 5.4 a). The XPS survey spectrum (Figure. 5.4 b) shows the presence of C, N and O in the Lyz-MgNCs. The peaks with binding energy of C 1s (284.4 eV, 286.9 eV and 287.7), N 1s (400 eV, 402.5 eV), and O 1s (531.0 eV, 532.1 eV) (Figure. 5.4 c, d) elements are probably due to the presence of lysozyme protein in Lyz-MgNCs and taken together, these data validate the successful synthesis of protein–magnesium nanocomplex and aligned with previously studied reported [85].

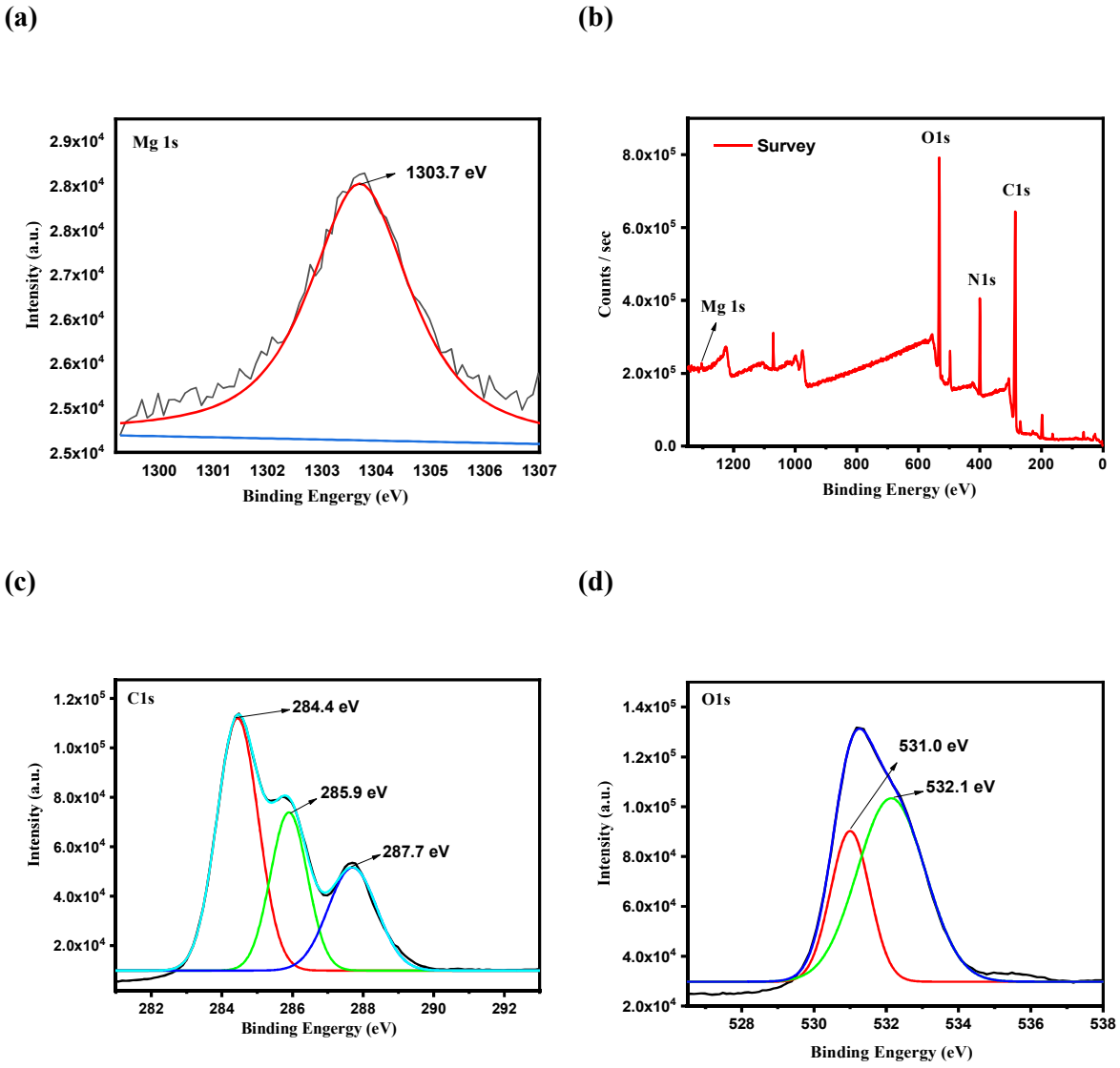

Figure.5.4 XPS spectra of Lyz-MgNCs (a) Mg 1s (b) survey spectra (c) C 1s (d) O 1s

5.4 Stability of Lyz-MgNCs

No discernible change in PL intensity was observed after adding different amounts of NaCl to freshly synthesized Lyz-MgNCs over a long period of time at 366 excitation (Appendix - Figure C 2 a) and 469 excitations (Figure. 5.5 a). This suggests that the Lyz-MgNCs can

withstand high ionic strengths with relative ease. However, as incubation period were increased, Lyz-MgNCs PL intensity was increased simultaneously.

(a) **(b)**

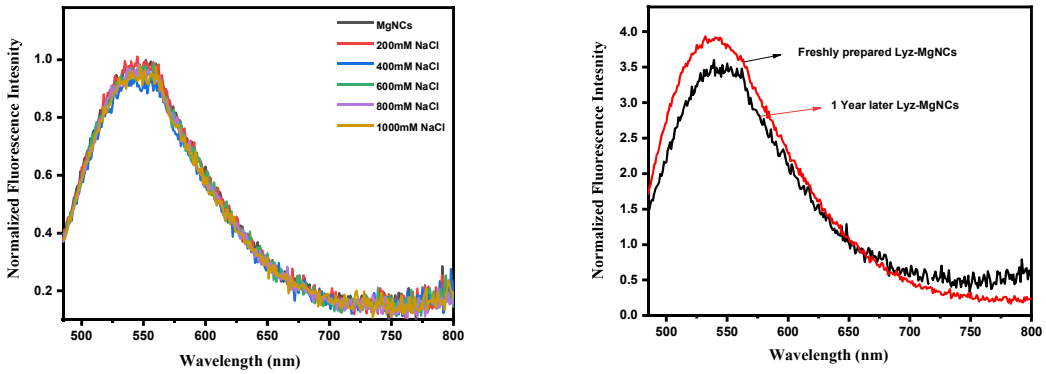

Figure.5.5 (a) Normalized fluorescence emission spectra of Lyz-MgNCs after addition of various concentration of freshly prepared NaCl solution at λ_{Ex} 469 (b) fluorescence emission spectra at 469 excitaion of freshly prepared Lyz-MgNCs and one year old Lyz-MgNCs.

The enhanced PL intensity may be attributed to an increase in the ligand to metal charge transfer (LMCT) that occurs as the surface Mg atoms of Lyz-MgNCs slowly oxidize. Even after being stored at refrigerator for one year, there was no discernible decrease in the PL intensity of Lyz-MgNCs was observed (Figure. 5.5 b). The synthesized Lyz-MgNCs can be preserved in vacuum dried solids forms, such as powder or film, obtained by after water removal. Further, the fluorescence emission of the solid film and powder exhibited the same emission characteristics as the original as-prepared solution, indicating the stability of the NCs in solid form. Consequently, the current method produced not only extremely luminescent Lyz-MgNCs, but also those that could be stored in solid form for prolonged use.

The strong interaction between the electron-donating groups of lysozyme protein and the magnesium core atoms, as well as the encapsulation and protection provided by high molecular weight lysozyme, are likely to be the primary sources of the increased stability of Lyz-MgNCs. The high temperature synthesis, which may improve the growth and digesting rate of NCs at the same time, may also contribute to the thermodynamic stability of Lyz-MgNCs. The stability of NCs can be influenced by the pH of surrounding solvent because change in pH can lead aggregation and dissolution of NCs, in our study we observed that prepared particles stable over a broad range pH stability (5.8-12) under 366 excitation (Appendix - Figure C 2 b) and 469 excitations (Figure. 5.6 a).

The photostability of nanoclusters is an important property for bioimaging applications. Consequently, photostability experiments were conducted to investigate the fluorescence behavior of Lyz-MgNCs under the Xe-lamp source (integrated into the spectrofluorometer) over an extended period of time and obtained data revealed that the emission intensity of the particles remained unchanged under continuous irradiation exposure for up to 83 minutes (Figure.5.6 b).

(a) **(b)**

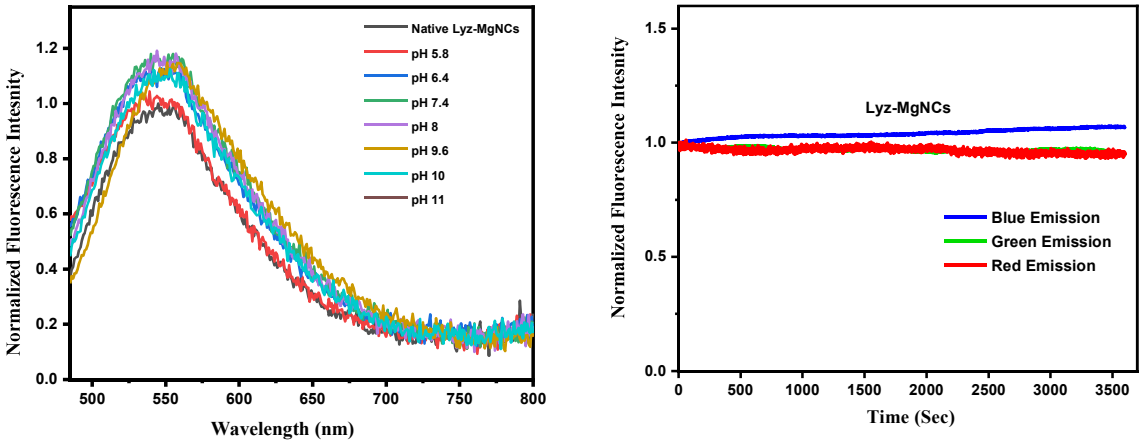

Figure. 5.6 (a) pH. Dependent Fluorescence emission spectra at different pH. (5.8-11) Values at λ_{Ex} 469 nm, (b) Photostability of Lyz-MgNCs at different excitations (366,469 and 560).

Furthermore, it was observed that the emission spectra of Lyz-MgNCs may not significantly change with the polarity or nature of the surrounding solvents such as DMSO, cyclohexane, acetone, ethanol, methanol with 366 excitations (Appendix – Figure. C 2 c) and 469 excitations (Figure. 5.7 a).

5.5 Application of Lyz-MgNCs

Before its applications as a bioimaging label, these nanoclusters were tested for cytocompatibility in U-87 MG cell lines, Following the cytocompatibility assay, Lyz-MgNCs were incubated with cell lines, and confocal images were acquired.

5.5.1 Cytocompatibility (MTT assay) and Bioimaging

Cytocompatibility assay is a crucial and foremost requirement for the administration of any material in real time. Effect of different concentration of Lyz-MgNCs on the cell proliferation and viability of U-87 MG cancer cells were determined by MTT assay (Figure.5.7 b).

Here, obtained result revealed that prepared clusters did not induced toxicity in the treated cells up to 90% at 1/10 ratio of stock concentration (12.4 mg/ml) as well as respective control of all nanoclusters are also biocompatible to the cells. Result represent that all nanoclusters found to be highly biocompatible in U-87 MG cells even higher concentration. Finally, results indicate that prepared nanoclusters are highly biocompatible and could be utilized for biological applications.

5.5.2 Blood Compatibility assay

Blood compatibility assessment is a crucial and foremost requirement for the administration of any nanomaterial *in vivo* such as haemolysis. The safety of the Lyz-MgNCs in the blood was assessed by the haemolytic assay (Figure. 5.7 c). The percent Haemolysis of the DI water, Saline and Lyz-MgNCs were 100 ± 9.897 %, 2.914 ± 0.60 % and 3.342 ± 0.061 %. The obtained results demonstrated that Lyz-MgNCs did not induce substantial haemolysis; i.e., they were hemocompatible at the concentrations used for the bioimaging and cell viability assay (1.25 mg/ml), which is comparable to previous research. Thus, the blood compatibility assay validated the potential of composites (and therefore Lyz-MgNCs) for in vivo applications [31].

(a) **(b)**

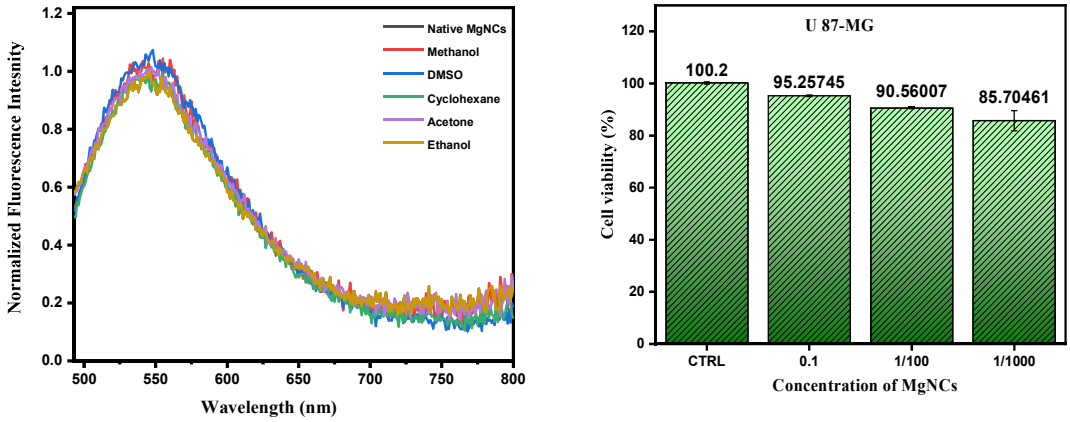

(c)

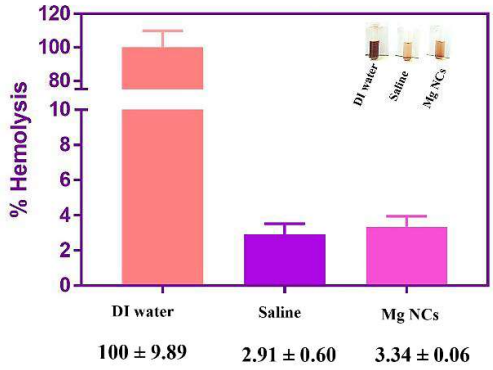

Figure.5.7 (a) Normalized fluorescence intensity of Lyz-MgNCs with different solvents at λ_{Ex} 469 nm (b) Cytotoxicity assessment in U-87 MG cells using MTT assay (c) Hemocomtability test of Lyz-MgNCs in rat blood.

5.5.3 Histopathology Results

In this study, the control group treated with normal saline solution did not exhibit any pathological lesions in the brain, lungs, liver, kidneys, and spleen. Likewise, no pathological lesions were observed in these organs for the Lyz-MgNCs-treated group at the 3-hour, 7-day, and 28-day time points (Figure. 5.8).

These findings suggest that the administration of Lyz-MgNCs was considered safe and non-toxic for *in vivo* administration [284].

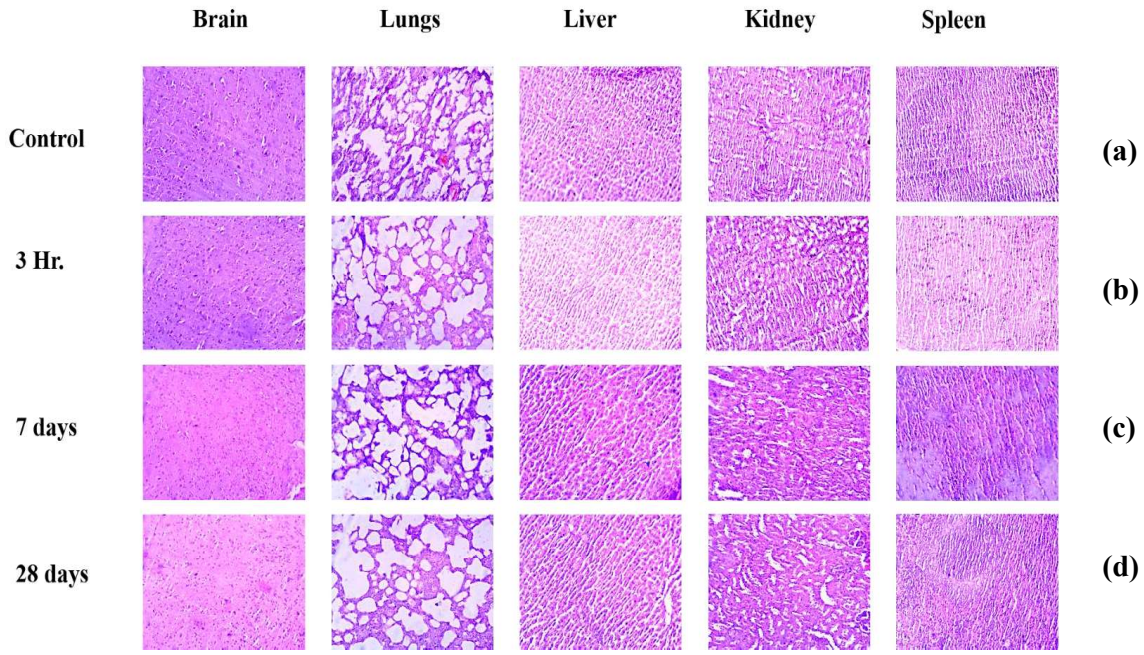

Figure. 5.8 Histopathological appearance in H & E-stained rat organ sections of all groups; (a) Normal tissue without injecting nanocluster (control group); (b) Tissue appearance (3 hrs) after injecting nanocluster through tail vein injection (c) Tissue appearance (7 days) after injecting nanocluster through tail vein injection, (d) Tissue appearance (28 days) after injecting nanocluster through tail vein injection. **Bar: 10 µm**

5.5.4 Clinical signs and body weight measurement

A careful examination of the rats before and after dosing of the Lyz-MgNCs suggested that there was absence of sign of the toxicity. Animal's behaviors were normal, movement inside the cage was normal, food intake was also normal. Additionally, we did not observe any sign of trauma and mortality. The body weight of the rats before and after dosing has been presented below.

Group	Before administration (gm)	2nd day (gm)	7th day (gm)	28th days (gm)
Control	240	241	238	242
	250	252	247	255
	255	254	250	257
Lyz-MgNCs	260	262	258	255
	245	247	250	254
	253	250	255	261

5.5.5 Cell Imaging

Lyz-MgNCs decorated with exceptional properties such as, negligible cytotoxicity, high fluorescence intensity, water solubility and excellent photostability, these features make them ideal candidate for cell imaging and labeling purposes. In our study, we incubated Lyz-MgNCs with human brain cell lines (U-87 MG) for 24 hrs. and visualized under confocal microscope, they showed bright, red, green and blue color fluorescence (Figure. 5.9), whereas, the control (Lysozyme protein) shows fluorescence only in blue region due to tryptophan residue, but the intensity is very low compared to Lyz-MgNCs (Appendix Figure C1). It was noticeable that the fluorescence signal occurred around the cytoplasm region rather than staining nucleus. This acquired data indicates that prepared Lyz-MgNCs can be utilized to stain living cells as well as visualize the real time cell tracking.

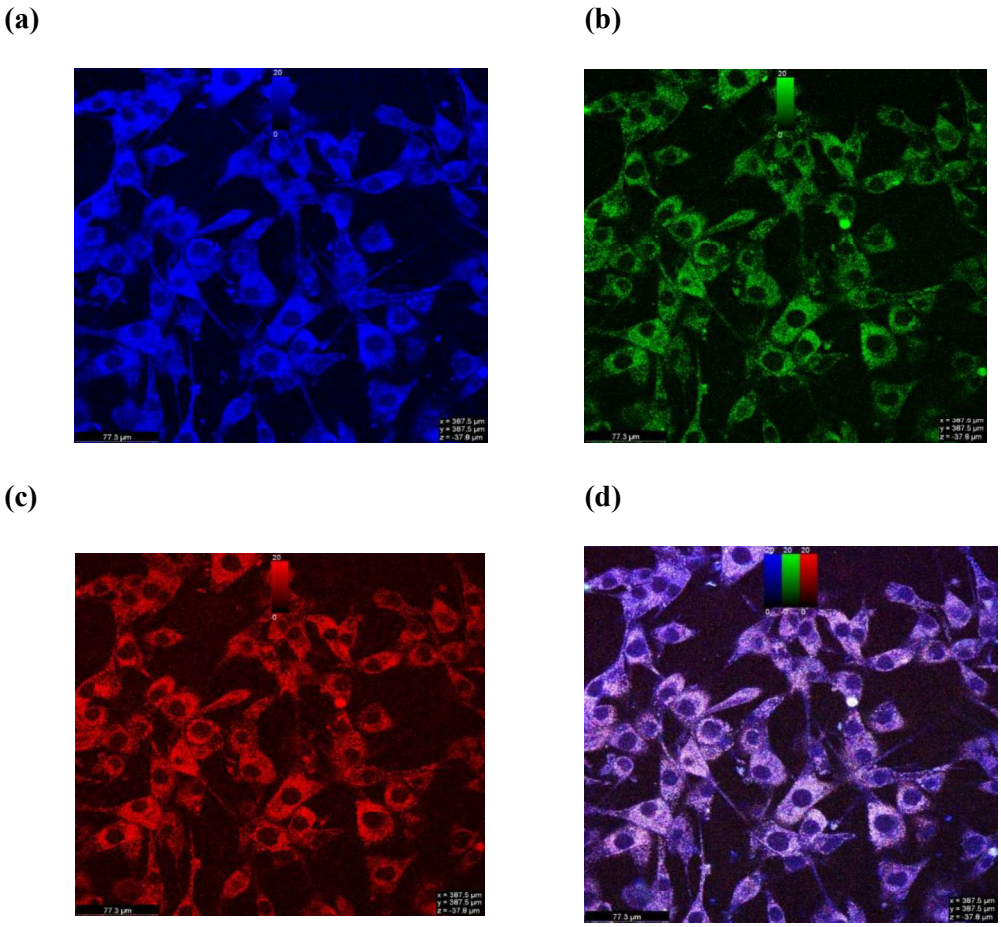

Figure. 5.9 Multifluorescent confocal image of U 87-MG cells incubated with Lyz-MgNCs (1/10 th of 12.4 stock solution) (a) Ex.366 /Em. 460 (b) Ex.472 nm / Em. Green (c) Ex. 472 nm / Em. Red (d) merged image. **Bar: 77.3 µm**

5.5.6 Confocal Z-stack analysis

Confocal Z-stack analysis was conducted to evaluate the mean fluorescent intensity of Lyz-MgNCs existing at different locations within the cell. This analysis involved examining different slices of the entire cell to understand their distribution within the cell. The cell was divided into 10 slices, each containing Lyz-MgNCs. Herein, 0 µm and 18 µm is abbreviated as lower and upper part of cell surface. Z-stack confocal cell images (10 slices) incubated with Lyz-MgNCs were acquired (Figure. 5.10 and Appendix- Figure.C3). With

an excitation wavelength of 366 nm and corresponding emission wavelength of 460 nm, the Mean fluorescent intensity was computed and analyzed at each slice within the cell surface. The analysis of the mean fluorescent intensity graph revealed that the highest intensity (100%) was observed at a distance of 6 μm above the lower surface of the cell, which indicated that the middle part of the cell surface exhibits the maximum fluorescence. The lowest intensity (35.07%) was observed at 18 μm, which represents the uppermost surface of the cell, which suggested that the topmost layer of the cell contains a lower concentration of nanoclusters, however in Figure. 5.10, 5.11 and 5.12's (k) represents the multifluorescent confocal image of U 87-MG cells treated with only Lysozyme in blue, green and red region. Therefore, for blue emitting Lyz-MgNCs, the mean fluorescent intensity patterns are shown as below: (a) = 90.09%, (b) = 92.13%, (c) = 96.37%, (d) = 100%, (e) = 95.91%, (f) = 85.49%, (g) = 84.5%, (h) = 94.35%, (i) = 78.30%, (j) = 35.07%.

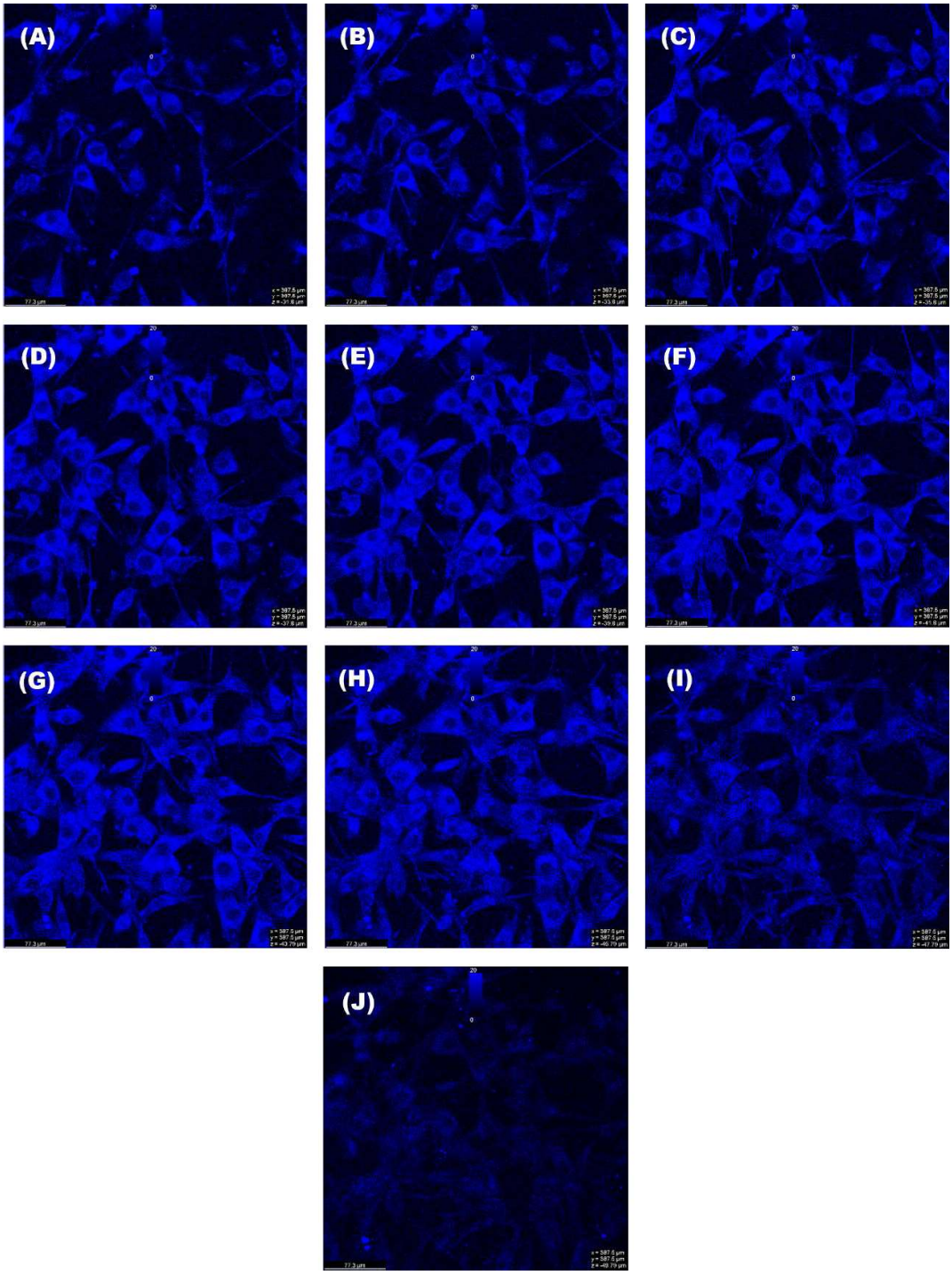

Figure.5.10 Z stack confocal images of U-87 MG cell incubated with Lyz-MgNCs (Ex. 366 nm, Em. blue). (a) = 0 µm. (b) = 2 µm. (c) = 4 µm. (d) = 6 µm. (e) = 8 µm. (f) = 10 µm. (g) = 12 µm. (h) = 14 µm. (i) = 16 µm. (j) = 18 µm.

In a similar manner, upon excitation at 460 nm wavelength with emission at 540 nm, the Mean fluorescent intensity was computed and analyzed at each slice within the cell surface. (Figure. 5.11) The analysis of the mean fluorescent intensity graph revealed that the highest intensity (100%) was observed at lower most part of the cell surface (0 μm), which indicated that the lower most part exhibits the maximum fluorescence intensity (Appendix-Figure. C4) The lowest intensity (5.45%) was observed at 10 μm, which represents the middle part of the cell surface, and subsequently showed low distribution of green emitting clusters in that particular region. Therefore, for green emitting Lyz-MgNCs, the mean fluorescent intensity patterns are shown as below: (a) = 100%, (b) = 74.94%, (c) = 95.76%, (d) = 92.04%, (e) = 86.59%, (f) = 85.49%, (g) = 5.45%, (h) = 97.33%, (i) = 67.28%, (j) = 49.85%.

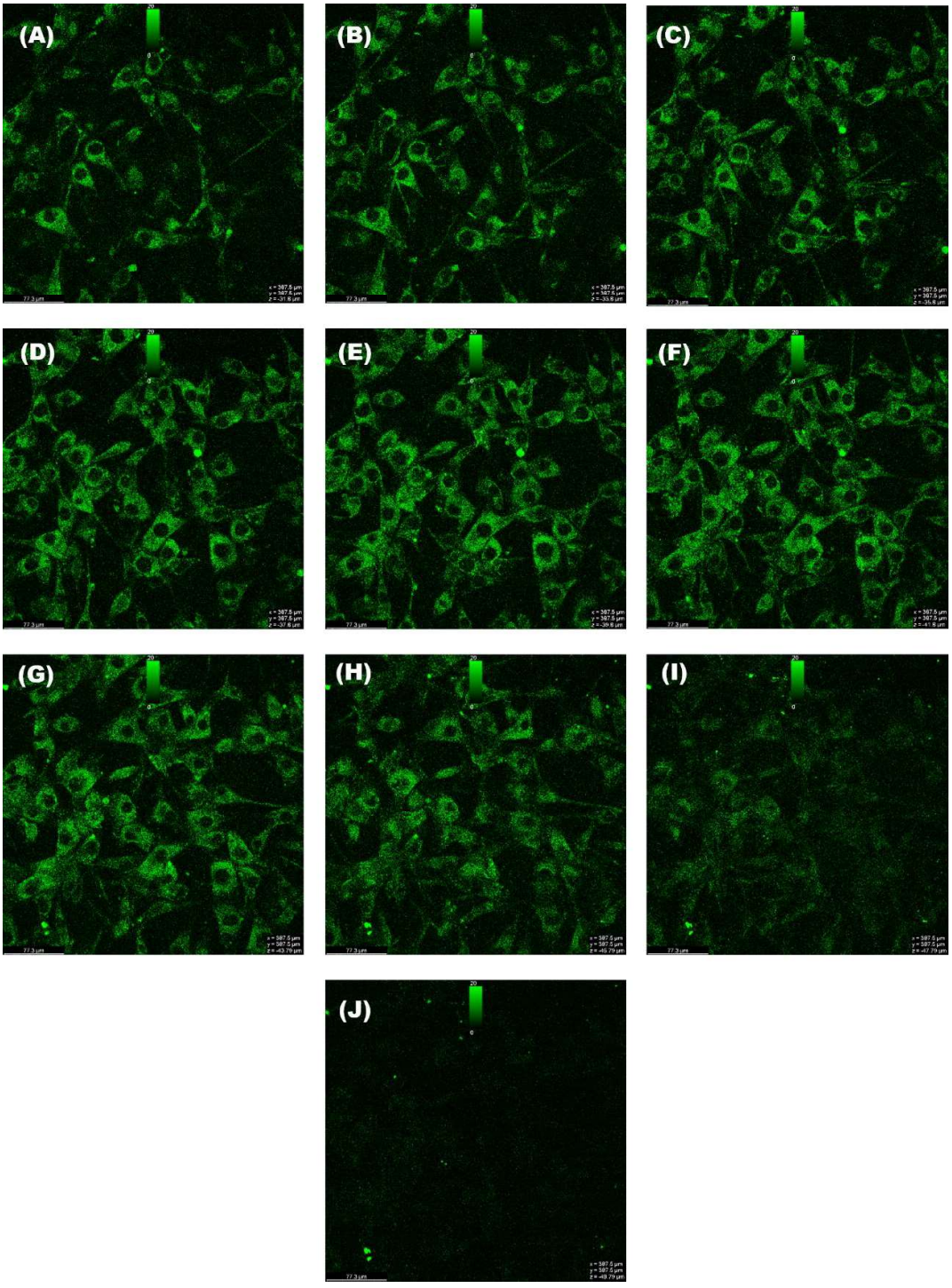

Figure.5.11 Z stack confocal images of U-87 MG cell incubated with Lyz-MgNCs (Ex. 460 nm, Em. green). (a) = 0 µm. (b) = 2 µm. (c) = 4 µm. (d) = 6 µm. (e) = 8 µm. (f) = 10 µm. (g) = 12 µm. (h) = 14 µm. (i) = 16 µm. (j) = 18 µm.

In another similar pattern, upon excitation at 560 nm wavelength with emission at 620 nm, the Mean fluorescent intensity was computed and analyzed at each slice within the cell surface. (Figure. 5.12 and Appendix- Figure. C5) The analysis of the mean fluorescent intensity graph revealed that the highest intensity (100%) was observed at lower most part of the cell surface (0 μm), which indicated that the lower most part exhibits the maximum fluorescence intensity. The lowest intensity (10%) was observed at 18 μm, which represents the upperpart of the cell surface, and subsequently showed low distribution of red emitting clusters in that particular region. Therefore, for red emitting Lyz-MgNCs, the mean fluorescent intensity patterns are shown as below: (a) = 100%, (b) = 96.25%, (c) = 93.26%, (d) = 91.66%, (e) = 89.87%, (f) = 79.08%, (g) = 90.84%, (h) = 90.68%, (i) = 66.84%, (j) = 10%. Upon comparing the results, it was observed that clusters of Lyz-MgNCs exhibited variations in size. The highest fluorescent intensity of blue emitting clusters was found at a distance of 6 μm above the cell surface, while for red emitting clusters, the maximum fluorescence intensity was observed at the lower part of the cell surface (0 μm). This indicates that the blue emitting clusters demonstrated the highest penetrability. However, for green and red emitting clusters, the lowest fluorescence intensity was observed at distances of 10 μm and 18 μm above the lower part of the cell, respectively. This reveals the presence of different levels of penetrability, although less penetrability compared to the blue emitting cluster.

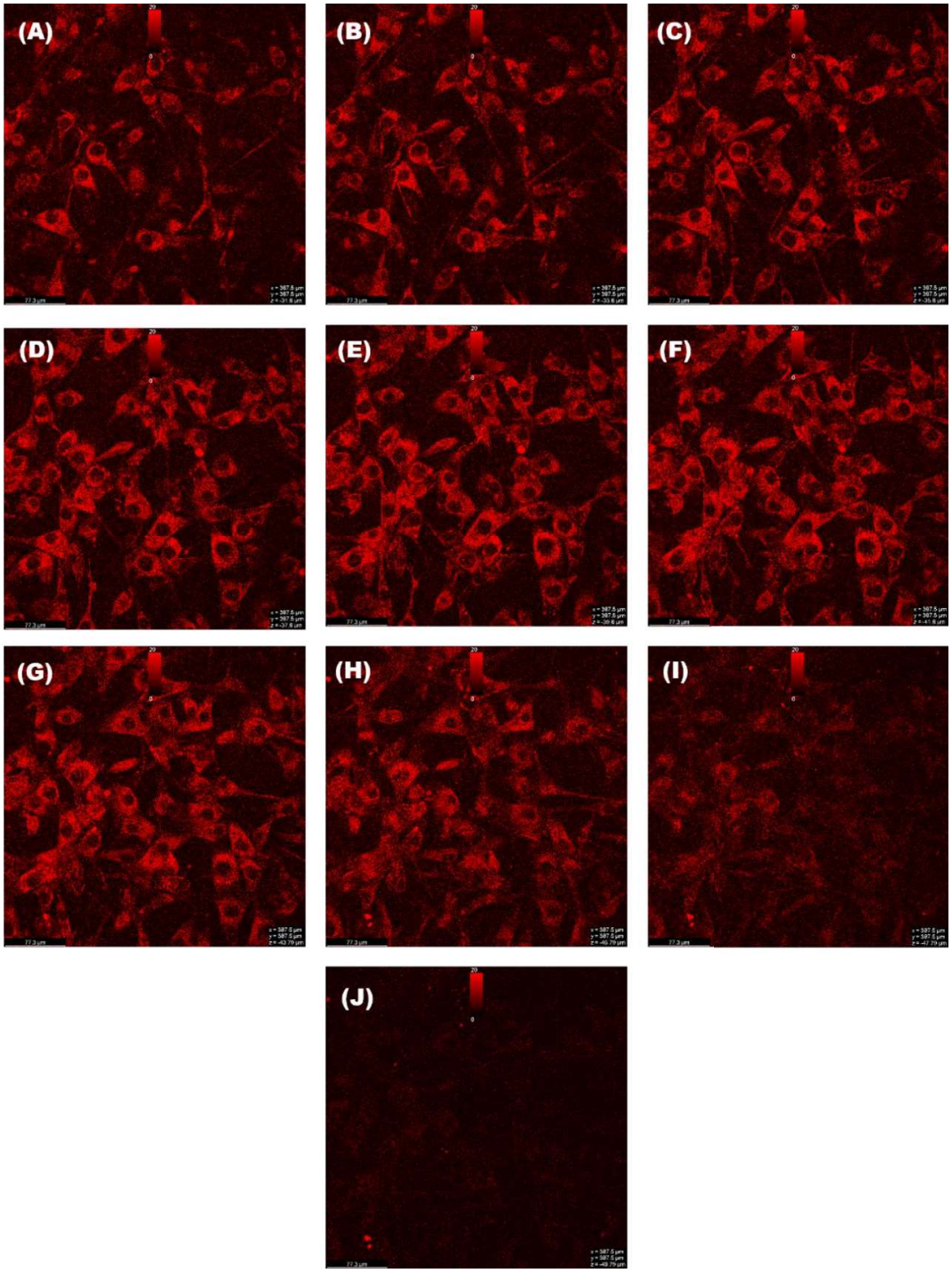

Figure. 5.12 Z stack confocal images of U-87 MG cell incubated with Lyz-MgNCs (Ex. 560 nm, Em. red) (a) = 0 µm. (b) = 2 µm. (c) = 4 µm. (d) = 6 µm. (e) = 8 µm. (f) = 10 µm. (g) = 12 µm. (h) = 14 µm. (i) = 16 µm. (j) = 18 µm.

5.5.7 In vivo biodistribution of the Lyz-MgNCs in the healthy mice

Figure.5.13 shows the results of the targeted imaging at 3 hours post injection, whole body fluorescence intensity of the mice injected with Lyz-MgNCs was captured. After 3 hours postinjection, Lyz-MgNCs distribution was observed in the vital organs of the mice such as brain, lungs, liver. This validates Lyz-MgNCs's *in vivo* imaging effectiveness, affirming its distribution within vital organs, signifying its potential as a tool for non-invasive visualization and tracking of substances within living organisms. Upon examination of the presented Figure 5.13, it is evident that the mice subjected to Lyz-MgNCs injection displayed a noteworthy increase in overall fluorescence intensity across their entire bodies. This fluorescence intensity, depicted graphically serves as a visual representation of the distribution pattern of the administered Lyz-MgNCs within the mice. Thus, the fluorescence intensity within these vital organs offers compelling evidence of Lyz-MgNCs's ability to traverse through biological barriers, potentially carrying implications for targeted delivery systems or diagnostic applications. In summary, the presented findings from the three-hour post-injection time point underline the effectiveness of Lyz-MgNCs as a fluorescent marker for *in vivo* imaging. Its discernible presence within key organs not only validates its distribution dynamics but also highlights its promise in advancing our understanding of substance movement within living organisms, opening avenues for diverse scientific and medical applications.

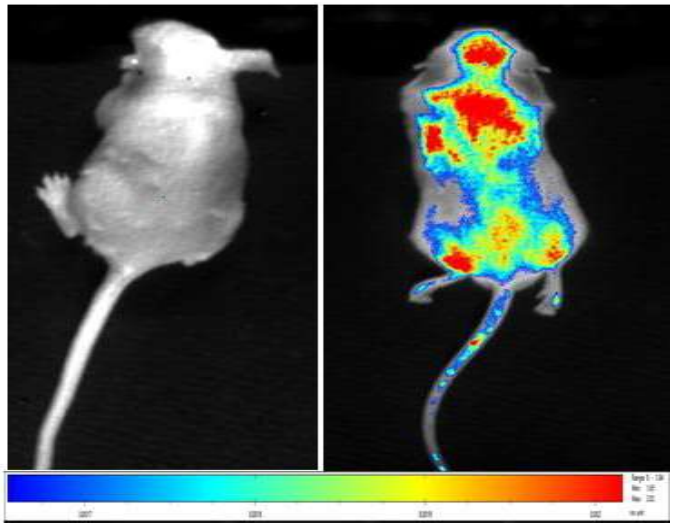

Control Treated with Lyz- MgNCs

Figure.5.13 Live animal fluorescent image after 3 h administration of saline in control mice and Lyz-MgNCs treated mice.

5.6 Ethical Clearance

The animal study protocols were approved by the Institutional Animal Ethics Committee (IAEC), IIT (BHU). IAEC Approval Number: IIT(BHU)/IAEC/2022/076. Registration no: 2123/GO/Re/S/21/CPCSEA).

5.7 Conclusion

In this work, we developed lysozyme-templated magnesium nanoclusters for bioimaging/biolabeling purposes. The surface Composition of Lyz-MgNCs makes it suitable for prolonged circulation with enhanced cellular uptake. The NCs showed high photoluminescence quantum yield, excitation-tunable fluorescence, high photostability, and colloidal stability. They could be used for labeling U-87 MG cells. In conjunction with the photoluminescence properties, their low cytotoxicity and biodegradability would make them an ideal candidate for biological and biomedical applications. The observed stability of the Lyz-MgNCs, coupled with the retention of fluorescence at physiological pH and in ionic solution (up to 1000 mM), is important for applications in vitro as well as in vivo. Confocal imaging in U-87 MG cells with CTCF analysis demonstrated their ability to deep penetration. The in-vivo investigation in terms of fluorescence retention and biocompatibility, demonstrated compelling evidence of Lyz-MgNCs ability to traverse through biological barriers and stain the organs without altering organs structural and functional integrity, Prepared Lyz-MgNCs potentially carrying implications for targeted delivery systems or diagnostic application